Myopathic Mutations Affect Differently the Inactivation of the Two Gating Modes of Sodium Channels

Oscar Moran,[1,2] Mario Nizzari,[1] and Franco Conti[1]

Three groups of mutations of the α subunit of the rat skeletal muscle sodium channel (rSkM1), homologous to mutations linked to human muscle hereditary diseases, have been studied by heterologous expression in frog oocytes: S798F, G1299E, G1299V, and G1299A, linked with potassium-aggravated myotonia (PAM); T1306M, R1441C and R1441P, linked with paramyotonia congenita (PC); T698M and M1353V, linked with the hyperkalemic periodic paralysis (HyPP). Wild-type rSkM1 channels (WT) show two gating modes, M1 and M2, which differ mainly in the process of inactivation. The naturally most representative mode M1 is tenfold faster and develops at ~ 30 mV less depolarized potentials. A common feature of myopathy-linked mutants is an increase in the mode M2 probability, P_{M2}, but phenotype-specific alterations of voltage-dependence and kinetics of inactivation of both modes are also observed. The coexpression of the sodium channel β_1 subunit, which has been studied for WT and for the five best expressing mutants, generally caused a threefold reduction of P_{M2} without changing the properties of the individual modes. This indicates that the mutations do not affect the $\alpha - \beta_1$ interaction and that the phenotypic changes in P_{M2} observed for the enhanced mode M2 behavior of the sole α subunits, although largely depressed in the native tissue, are likely to be the most important functional modification that causes the muscle hyperexcitability observed in all patients carrying the myotonic mutations. The interpretation of the more phenotype-specific changes revealed by our study is not obvious, but it may offer clues for understanding the different clinical manifestations of the diseases associated with the various mutations.

KEY WORDS: Heterologous expression; oocytes; modal gate; skeletal muscle; paramyotonia congenita; hyperkalemic periodic paralysis; potassium aggravated myotonia.

INTRODUCTION

Sodium channels are the integral membrane proteins responsible for the initial phase of the action potential in excitable cells (Hille, 1992). In the skeletal muscle fiber, sodium channels are essential for the propagation of the action potential along the cell surface and in the T-tubules, leading the events that ultimately trigger muscle contraction. Anomalies in the adult skeletal muscle voltage-gated sodium channels (SkM1) can have important consequences for muscle physiology and cause pathological conditions (Barchi, 1995; Cannon, 1996a). This is exemplified by a group of autosomal dominant hereditary muscle diseases, including paramyotonia congenita (PC), potassium-aggravated myotonia (PAM), and hyperkalemic periodic paralysis (HyPP), whose symptoms can be attributed to hyperexcitability of the sarcolemma (Cannon, 1996b; Hoffman *et al.*, 1995). To date, 21 different point mutations of the SCN4A gene, located in chromosome 17q (23.1 to 25.2) and coding for the human SkM1 α subunit, have been linked with so-called muscle sodium channelopathies (Bulman, 1997). The mutations are all in the coding regions of the gene and

[1] Istituto di Cibernetica e Biofisica, CNR, Via De Marini, 6, I-16149 Genova, Italy.

[2] Author to whom all correspondence should be sent. Email: moran@barolo.icb.ge.cnr.it.

are produced by transversion of single nucleotides that cause substitutions of highly conserved residues. The key manifestations of a muscle sodium channelopathy are stiffness and weakness. Symptoms are variable between affected members of the same family (DeSilva *et al.*, 1990) and with even greater clinical differences between unrelated individuals carrying the same mutation (Cannon 1996b). Electrophysiology on muscle specimens from such patients revealed a small deficiency in the inactivation of the sodium currents as a typical abnormality (Cannon *et al.*, 1991; Lehmann-Horn *et al.*, 1991; Lerche *et al.*, 1993; Lerche *et al.*, 1996; Tahmoush *et al.*, 1994). As the functional properties of these mutations are difficult to isolate in native muscle fibers, many groups have studied the heterologous expression of the hSkM1 α subunit in cDNA-transfected mammalian cells or in cRNA-injected frog oocytes. In all cases, the primary defect is some impairment of the "normal" sodium channel inactivation seen either as persistent currents at the end of relatively long depolarizations, or as a slower decay of the transient current, or as a positive shift in the voltage dependence of inactivation, or as some combination of these effects (see Barchi, 1995; Cannon, 1996a, b; Hoffman *et al.*, 1995 for reviews). Both animal (Cannon and Corey, 1993) and theoretical (Cannon *et al.*, 1993a; Green *et al.*, 1998; Moran *et al.*, 1998a) models have demonstrated that even low levels of this type of inactivation defects can cause myotonia and/or paralysis. Thus, the phenotype–genotype correlation is likely to mainly involve the specific type of inactivation defect caused by each mutation.

Unlike the sodium currents expressed by mammalian cells transfected by the SkM1 α subunit, which closely resemble those of native muscle fibers, the expression of the sole α subunit in oocytes shows an abnormally high component of a slowly inactivating mode (Auld *et al.*, 1988; Moorman *et al.*, 1990; Moran *et al.*, 1998a; Trimmer *et al.*, 1989; Zhou *et al.*, 1991). This slowly inactivating mode is substantially reduced by coexpression of the β_1 subunit (Ji *et al.*, 1994; Moran *et al.*, 1998b; Patton *et al.*, 1994; Zhou *et al.*, 1991). The fairly normal expression of the slow mode in transfected cells is probably due to an endogenous expression of the sodium channel β_1 subunit (Mitrovic *et al.*, 1994). The exacerbation of the slow mode in oocytes makes this system more appropriate for studying the modal gating of the channel (Moran *et al.*, 1998b). In the present study, we have exploited this fact and, wherever possible, have compared the results of the expression in frog oocytes of the α subunit

alone, or the coexpression of the α and β_1 subunits. As a template for our studies of wild-type and mutant phenotypes, we have used the adult rat skeletal muscle sodium channel (rSkM1, μ1), which has more than 90% identity with the human one. In this work, we compare the properties of the fast (M1) and slow (M2) modes of inactivation of the wild phenotype (WT) with those of four PAM-linked mutations (S798F, G1299E, G1299V, and G1299A, corresponding to human mutations S804F, G1306E, G1306V, and G1306A), two HyPP-linked mutations (T698M and M1353V, corresponding to human mutations T704M and M1360V), and three PC-linked mutations (T1306M, R1441C, and R1441P, corresponding to human mutations T1313M, R1448C, and R1448P). We find that these mutations change the voltage dependence and the kinetics of inactivation of both modes, besides increasing the intrinsic propensity of the α subunit, the pore-forming polypeptide, for the slower mode. The coexpression of the β_1 subunit, studied for the most highly expressing mutants, was found to merely decrease the probability of the slow mode by a phenotype-independent factor. The phenotypic differences in the inactivation properties are consistent with the different clinical manifestations and the severity of mutation-linked disorders.

MATERIALS AND METHODS

Mutagenesis

The full-length cDNA coding for the rSkM1 sodium channel α subunit (Trimmer *et al.*, 1989) was subcloned into the *EcoRI* site of the prokaryotic vector pGEMHE containing the 5′–3′ untranslated β-globin sequence that induces a high expression in frog oocytes (Liman *et al.*, 1992). Site-directed mutagenesis was accomplished using the *Pfu* DNA polymerase (Kudel, 1985; Sugimoto *et al.*, 1989) using the QuikChange kit (Stratagene). For each mutant, we designed two mutagenic primers (M-Medical, Florence), each complementary to the opposite strands of the vector that extend during temperature cycling by means of the Pfu DNA polymerase. The *DpnI* endonuclease, specific for methylated DNA, was used to digest the parental DNA template. The mutations were verified by sequencing 400 bp's in the flanking region near the mutagenic point by dideoxynucleotides methods (Sanger *et al.*, 1977).

The plasmids containing the wild-type (WT) or mutant cDNA were linearized with *NheI*. Plasmids

containing the cDNA coding the rat sodium channel β_1 subunit (psPNa-β, generous gift from K. Imoto) were linearized with *EcoRI*. Linearized plasmids were transcribed *in vitro* with T7 polymerase at 37°C for 2 h, using the capped mMessage mMachine kit (Ambion). After digesting the DNA template with DNase I, cRNA was precipitated in LiCl. The pellet was washed with 70% ethanol, resuspended in DEPC-treated water, and stored at −80°C for further use.

Sodium Channel Expression

Oocytes were surgically extracted from anesthetized *Xenopus laevis* frogs and isolated enzymically by treating the ovarian tissue for 1.5–2 h at room temperature with a Ca^{2+}- and Mg^{2+}-free Barth's solution containing 1 mg/ml of collagenase A (Sigma). Stage IV and V oocytes were injected with 50 nl of 125 to 250 ng/µl solutions of cRNA in DEPC water. In some experiments, the α-cRNA was co-injected with β_1-cRNA. Injected oocytes were incubated for 4 to 6 days in Barth's solution at 18°C (Stühmer, 1992).

Electrophysiological Recording

Sodium currents were measured from membrane macro patches in the cell-attached configuration (Hamill *et al.*, 1981; Stühmer, 1992) using an Axopatch-200B patch-clamp amplifier (Axon Instruments). Aluminium silicate glass micropipettes (Hilgemberg) were coated with silicone rubber and fire polished to a tip diameter yielding a resistance of 0.6 to 1.2 MΩ in the working solutions. The pipette was filled with normal frog Ringer (in mM: NaCl 115, KCl 2.5, $CaCl_2$ 1.8, HEPES 10; pH = 7. 4). The oocyte bathing solution had the following composition (in mM): KCl 120, Tris-Cl 20, EDTA 5; pH 7.4. Because of the high potassium concentration of the bath solution, the cell membrane potential was 0 $\pm$ 2 mV. Therefore, the membrane patch potential, V, was estimated to be just opposite to the pipette potential. The output of the patch-clamp amplifier was filtered by the built-in low-pass 4-pole Bessel filter with a cut-off frequency of 5 kHz and sampled at 20 kHz. The membrane patch was kept at a holding potential of −120 mV. Pulse stimulation and data acquisition used 16 bit D–A and A–D converters (ITC-16, Instrutech) and were controlled by a Macintosh microcomputer with the Pulse software (Heka Electronik). Linear responses were estimated from subthreshold stimulations, partially compensated analogically, and digitally subtracted with a standard P/4 protocol. All measurements were done at a controlled temperature of 15 $\pm$ 0.5°C.

Data Analysis

Data were analyzed with a Macintosh microcomputer using PulseFit (Heka Electronik) and custom software developed in the Igor program (Wavemetrics). Statistical comparisons were done with a Student's *t*-test, and statistical significance was defined by $p < 0.05$. The results were expressed as mean $\pm$ sem (number of measures). A simplex method was used for curve fitting. Data for WT and for each mutant channel were obtained from two to four different batches of oocytes.

RESULTS

All the prepared constructs expressed sodium currents, although the mutations yielded average smaller current amplitudes. The maximum peak current measured within 3–4 min after having obtained the gigaseal was 800 $\pm$ 300 pA (mean $\pm$ sem; $n = 11$) for WT. Lower expression levels were found for G1299V (600 $\pm$ 130 pA; $n = 8$), M1353V (470 $\pm$ 80 pA; $n = 12$), T698M (340 $\pm$ 60 pA; $n = 8$), T1306M (330 $\pm$ 70 pA, $n = 11$), S798F (290 $\pm$ 150 pA; $n = 9$), G1299A (280 $\pm$ 80 pA; $n = 13$) and R1441C (230 $\pm$ 60 pA, $n = 14$), and the lowest expression level ($p < 0.05$) was found for the mutants R1441P (120 $\pm$ 20 pA; $n = 14$), and G1299E (90 $\pm$ 12 pA, $n = 7$). In most cases, peak currents increased two- to three-fold during the first 10 min of experiments and achieved fairly stable levels only after about 20 min.

Variability of Results

As previously reported (Moran *et al.*, 1998a, c), there is a considerable variability in the voltage dependence of the sodium currents mediated by the same type of channel and measured from different batches of oocytes, or different oocytes from the same batch, or even different patches of the same oocyte. Most of this variability appears to be due to changes of surface potentials, as indicated by the fact that the potential

that activates 50% of the maximum peak conductance, $V_{1/2}$, varies during a single experiment (Fig. 1A). A negative shift of 5 to 40 mV was found in most experiments within 20–30 min from the first recording on a single patch. Similar artefacts have been reported also for recordings from HEK 293 cells permanently transfected with rSkM1 channels (Cummins and Sigworth, 1996) or from cardiac muscle fibers (Wend *et*

al., 1992). It has been recently suggested that this phenomenon is due to a disturbance of the channel–cytoskeleton interactions caused by the local mechanical stress associated with the patch isolation (Shcherbatko and Brehm, 1998).

To avoid this problem, we decided to use an "internal" reference potential for each experiment, in a way similar to that used for macroscopic voltage-
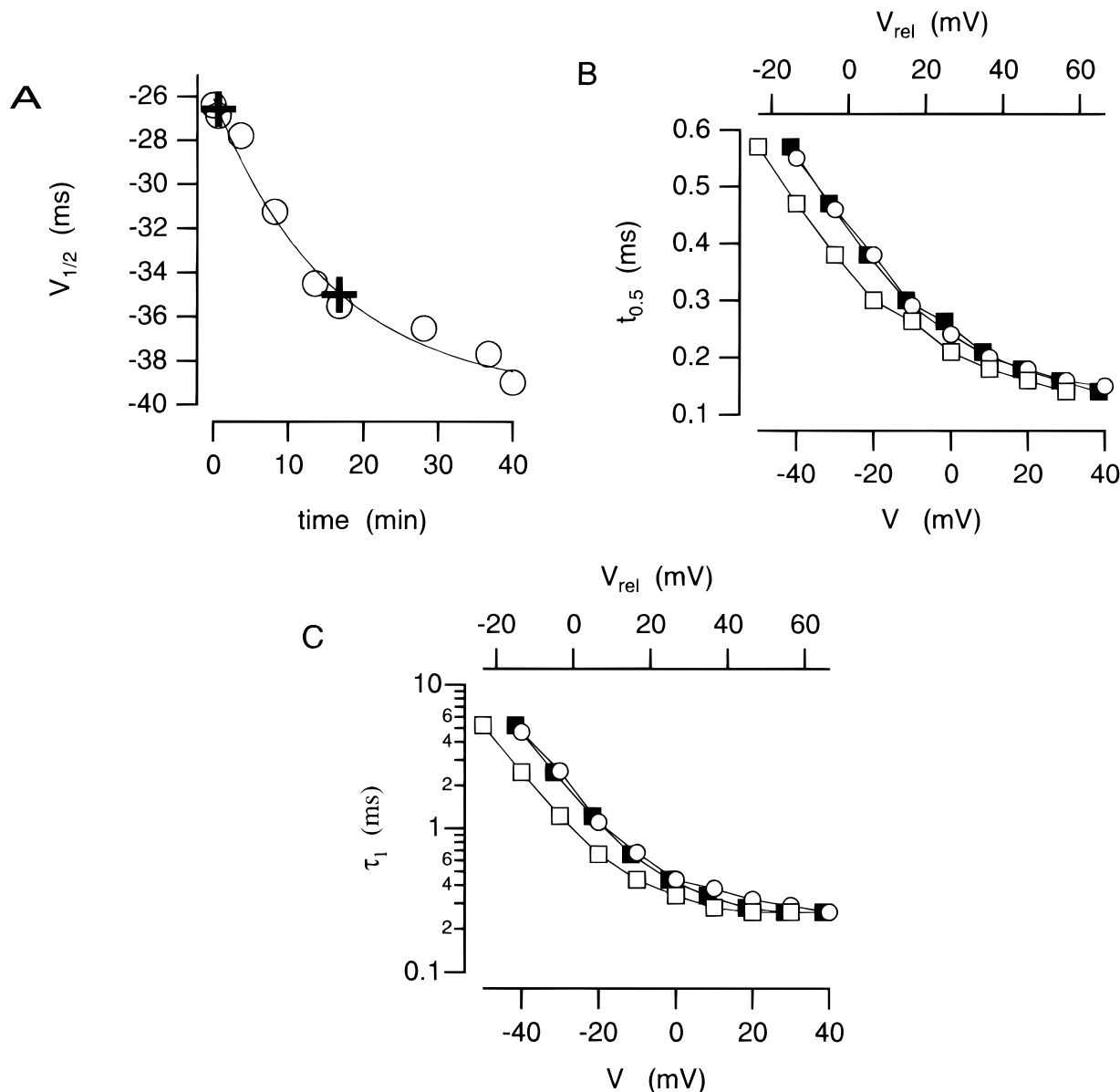

Fig. 1. Correction of the kinetic parameters of the sodium channel by the half-activation potential, $V_{1/2}$. Data was obtained from WT channels. (A) The $V_{1/2}$ values, estimated along a 40-min experiment, were plotted against time, and interpolated with an exponential function. (B) and (C) are, respectively, the time to one half of the maximum amplitude, $t_{0.5}$, and the fast inactivation time constant, τ_1 (open symbols) values measured at times indicated by crosses in (A) and plotted against the potential (lower axis). Observe that the shift in the time constants, which occurred in 17 min (filled symbols), is corrected by replotting the values against the V_{rel}, represented in the upper axis (fill symbols).

clamp measurements in the node of Ranvier, where the steady-state half-inactivation potential is used as a reference potential (see Stämpfli and Hille, 1976). We have chosen as a reference the value of $V_{1/2}$, measured periodically and systematically during each experiment, because the main effect of the myopathic mutations studied appears to be on the inactivation properties of the channel. Furthermore, in agreement with previous reports (Ji *et al.*, 1994; Moran *et al.*, 1998a), we found no significant differences in the activation curves of the two gating modes measured on the same patch at the same time intervals, so we do not expect that $V_{1/2}$ is affected by changes in modal propensity. Figure 1A shows the time course of $V_{1/2}$ estimated from standard I–V protocols, during a representative experiment on WT channels, showing a shift of the activation curve by about-15 mV in 40 min. The time course of $V_{1/2}$ was well fitted by an exponential function. Figures 1B and C show plots of the voltage dependence of half-activation time, $t_{0.5}$, and the time constant of fast inactivation, τ_1, as measured at the beginning of the experiment (circles), and after 17 min (squares). It is seen that the voltage dependence of both of these kinetic parameters are shifted by about -10 mV, the same change observed in the values of $V_{1/2}$ measured at the same times (crosses in Fig. 1A). Thus, when expressed in terms of V_{rel}, the two sets of data superimposes (filled symbols in Fig. 1B and C). Using this type of characterization, we find full superposition of voltage-dependent data obtained at different times during an experiment and we have much more confidence in the comparison of the results obtained from different experiments.

Bimodal Gating of Channels

Following a step depolarization from a holding potential $V_h = -120$ mV, the sodium current mediated by the expression in oocytes of the α-rSkM1 channel show a fast activation and a biphasic inactivation, as shown in Fig. 2A (Ji *et al.*, 1994; Moorman *et al.*, 1990; Moran *et al.*, 1998a; Zhou *et al.*, 1991). The falling phase of the current can be well fitted with a double-exponential function as $I(t) = a_1 e^{(-t/\tau_1)} + a_2 e^{(-t/\tau_2)}$, with fast and slow time constants, τ_1 and τ_2, differing by about one order magnitude, and with a ratio of the two amplitudes a_1 and a_2 fairly independent of the depolarizing voltage. It has been proposed that the two components are due to the separate contribution of a mixed population of channels, that, at the time of the stimulus, are either in a fast or in a slower
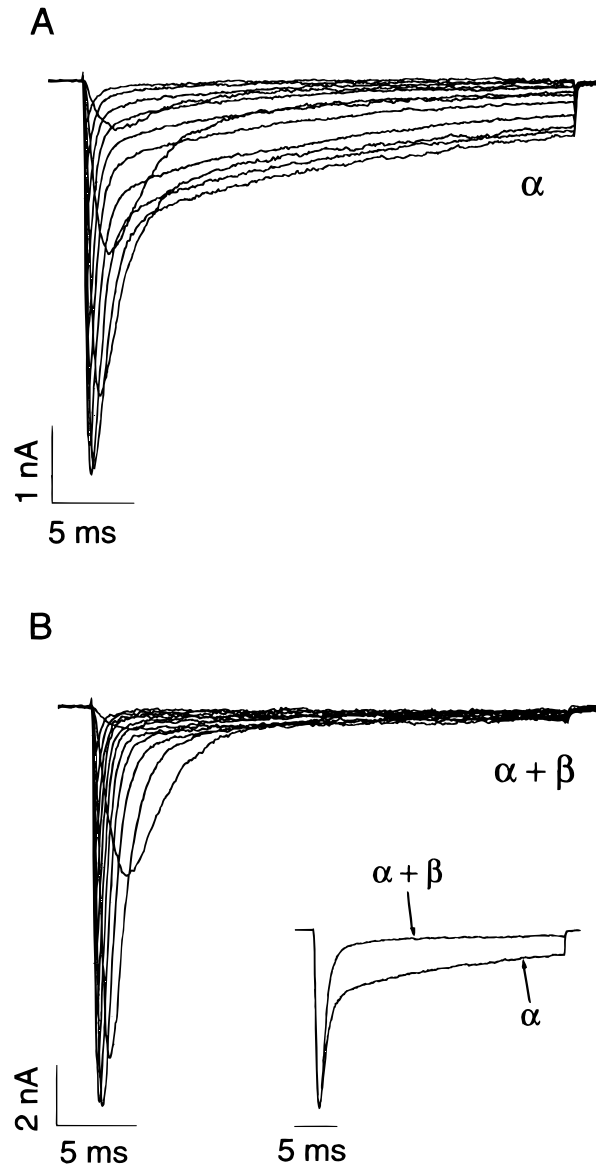

Fig. 2. Sodium currents recorded in *Xenopus oocytes* WT sodium channel α subunit (A) and coexpressing α and β_1 subunits (B). Currents were elicited by 20-ms depolarizing pulses from a holding potential of -120 mV to a test potential between -50 and 50 mV in 10-mV steps. The inactivating phase of currents expressed by the sole α subunit are characterized by two time constants. A significant reduction of the slower component of the current is observed when the β_1 subunits coexpressed with the α subunit. The inset is the comparison between the currents expressed with and without the β_1 subunits, measured near to the half-activation potential (± 5 mV), and scaled to the peak of the current.

mode of inactivation. Single-channel recordings have shown that in the fast inactivating mode, which we shall call M1, the channels open once and briefly during the depolarizing stimulus. In the slower mode,

called M2, channels have late reopenings during the sweep (Moorman *et al.*, 1990; Patton *et al.*, 1994; Zhou *et al.*, 1991; Chang *et al.*, 1996).

To quantify the propensity of the channels to gate either mode, we defined the parameter $P_{M2} = a_2/(a_1 + a_2)$, as a measure of the probability of finding a channel in mode M2 during any test stimulus. P_{M2} was measured from the double-exponential fit of the decaying phase of the sodium current evoked by 30 to 150 ms depolarization to voltages between -20 and $+40$ mV. The M2 component of sodium currents expressed in oocytes by WT α subunits (Ji *et al.*, 1994; Moorman *et al.*, 1990; Trimmer *et al.*, 1989) is more pronounced than in cDNA-transfected mammalian cells (Ukomadu *et al.*, 1992), where less than 2% of the channels gate in mode M2, probably because of endogenous expression of a β_1 subunit (Mitrovic *et al.*, 1994). Consistent, with these reports, we found that the expression of the WT α subunit showed on average about 10% of slowly inactivating currents ($P_{M2} = 0.1 \pm 0.02$; $n = 15$), whereas the M2 propensity in oocytes was reduced to less than one third ($P_{M2} = 0.03 \pm 0.01$; $n = 21$), when the α subunit was coexpressed with the β_1 subunit (see Fig 2B).

Figure 3 shows representative records of the currents in response to step depolarizations to near $V_{1/2}$ for all the mutants studied. The record obtained from a representative WT experiment is shown in each panel for comparison, scaled to the same peak amplitude. We have systematically observed that the slowly inactivating component of the currents mediated by mutant channels is more pronounced than that of WT. As clearly seen in Fig. 3, it results in the fact that mutant channels have much larger late current at the end of pulses of 25-ms duration. Significantly larger values of P_{M2} ($p < 0.02$), by a factor between 2 and 4 were found for all the mutant channels studied in comparison to WT, as shown in Table I. Similar to what we have previously reported for the PC mutant T1306M (Moran *et al.*, 1998b), the coexpression the in the PAM mutants G1299E, G1299V, and G1299A or the HyPP mutant T698M reduced P_{M2} by about the same factor of 3 as it did with the WT (Table I). Coexpression of the β_1 subunit does not significantly change the voltage dependence and kinetics of each mode (data not shown). This suggests that the main effect of the α–β_1 interaction is a reduction of the propensity of the channels for mode M2 by a phenotype-independent factor and is consistent with observations in preparations showing smaller values of P_{M2}, like in mammalian cells transfected with rat or human SkM1 α subunit.
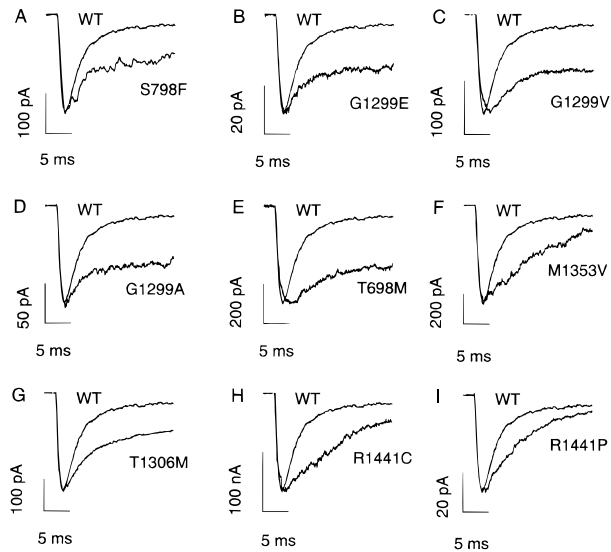

Fig. 3. (A–I) Sodium currents expressed in *Xenopus* oocytes microinjected with WT and mutant cRNA coding the α subunit of rSkM1 sodium channels. Currents were elicited by 20 ms depolarizing pulses from a holding potential of -120 mV to a test potential between near to the half-activation potential (± 5 mV). A record of the WT channel scaled to the peak of the current is included on each panel for comparison. Observe the significant increase of the slow inactivating component of the current in all mutants.

In these preparations, a similar increase of the slower mode of inactivation (usually expressed as the ratio between late current and peak current) has been described on the equivalent PAM mutations S798F (Green *et al.*, 1998; Moran *et al.*, 1998c) G1299E, G1299V (Hayward *et al.*, 1996; Mitrovic *et al.*, 1995), and G1299A (Hayward *et al.*, 1996; Mitrovic *et al.*, 1995), for the HyPP mutations T698M (Cannon and Strittmatter, 1993; Cummins and Sigworth 1996; Cummins *et al.*, 1993) and M1353V (Cannon and Strittmatter, 1993), and for the PC mutations T1306M (Hayward *et al.*, 1996), whereas no significant increase in the late current has been reported for the G1299A mutation (Mitrovic *et al.*, 1995). These data are compatible with measurements done in human muscle fibers from patients with the equivalent mutations G1306E, G1306V, and G1306A (Lerche *et al.*, 1993), T1313M (Tahmoush *et al.*, 1994), and R1448P (Lerche *et al.*, 1996).

Inactivation Kinetics

As described above, the decaying phase of the sodium currents can be well fitted with a double-expo-

nential function. We have systematically fitted the currents evoked by 30-ms pulses to membrane potentials between -30 to 30 mV (corresponding to V_{rel} in the range of -20 mV $\div$ 60 mV, depending on the value of $V_{1/2}$ for each experiment). In some cases, the fast component of the current was too small and could not be reliably dissected, in particular, at low membrane potentials. To overcome this inconvenience, we attempted to separate the two gating modes with an appropriate conditioning protocol, that reduced the amplitude of the M2 component of the current (Moran *et al.*, 1998a). The rationale of this protocol is described in the Fig. 4. A depolarizing test pulse to $V \geq -20$ mV from $V_h = -120$ mV elicits sodium currents contributed by channels gate in either the two modes, M1 or M2 (Fig. 4A). However, a conditioning prepulse to 0 mV for 100 ms causes a complete inactivation of all channels, that is not removed by a brief repolarization of 0.5 ms at -120 mV (Fig. 4B). A significant recovery from inactivation of the channels that are in mode M1 is obtained after relatively short repolarizations (see, for example, the second trace of Fig. 4B obtained after 2.5 ms at -120 mV), and most of the channels in mode M1 are available for activation after 16 ms (third trace of Fig. 4B). Only after much longer repolarizations (e.g., 128 ms in the Fig. 4B), have the channels gating in mode M2 recovered from inactivation. Subtracting from the unconditioning response the trace obtained after intermediate repolarization periods (16 ms), that retrieve from the inactivated state most of the channels in mode M1, the slower component due to channels in mode M2 becomes evident (Fig. 4C). Rather than trusting the full reliability of this type of dissection, we used conditioning prepulses just for estimating the time constants of inactivation in mode
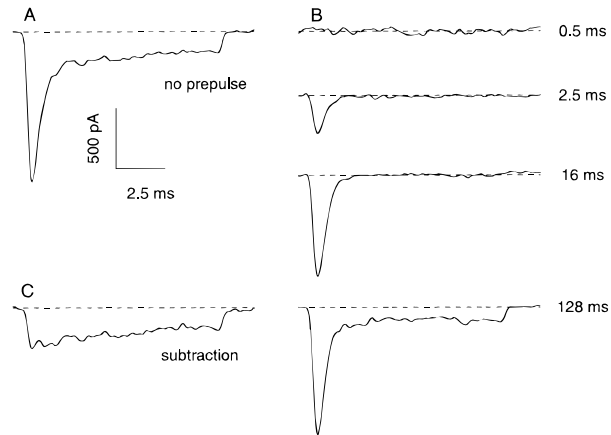

Fig. 4. Dissection of the two gating modes is based on their very different rates of recovery from inactivation. (A) Sodium current with a holding potential of -120 mV and a test pulse to -20 mV, showing the two gating modes. (B) When the test pulse is preceded by a conditioning pulse to 0 mV for 100 ms, followed by a repolarization to -120 mV of various durations (as indicated), recovery of M1 mode is almost complete in $\sim$20 ms, whereas M2 has twentyfold slower recovery. A repolarization of 0.5 ms is not enough to remove any inactivation. A partial recovery of M1 mode is obtained for 2.5 ms repolarization, while the recovery of M1 mode is almost complete in 16 ms, when M2 is still practically undetectable. Channels recover from M2 mode inactivation only by much longer repolarizations (128 ms). (C) M2 mode contribution is obtained by subtraction of the trace in (A) and the 16-ms repolarisation in trace in (B), which contains only the M1 mode contribution.

M1, τ_1, and we then fitted the no-conditioned current records using τ_1 as a fixed value of the fast time constant. The reliability of this strategy was checked in cases in which the unconditioned responses had a relatively large fast component: Estimates of τ_1 obtained from conditioned records or from the double-exponential fit of the unconditioned record with τ_1 as

Table I. Propensity of Mode M2 (P_{M2}) in Membrane Patches from Oocytes Expressing Wild-Type and Mutant rSkM1 Channel α Subunit and Coexpressing the α and β Subunits[a]

		α Subunit	p	$\alpha + \beta$ Subunits	p
	Wild type	0.11 ± 0.02 (15)	—	0.03 ± 0.01 (21)	—
PAM	S798F	0.47 ± 0.07 (8)	< 0.00001		
	G1299E	0.35 ± 0.05 (12)	< 0.0002	0.06 ± 0.02 (5)	N.S.
	G1299V	0.23 ± 0.04 (13)	< 0.02	0.06 ± 0.01 (8)	< 0.05
	G1299A	0.39 ± 0.06 (12)	< 0.0002	0.07 ± 0.02 (5)	N.S.
HyPP	T698M	0.28 ± 0.05 (14)	< 0.005	0.07 ± 0.03 (6)	N.S.
	M1353V	0.23 ± 0.05 (12)	< 0.05		
PC	T1306M	0.44 ± 0.05 (10)	< 0.00001	0.13 ± 0.02 (8)	< 0.0002
	R1441C	0.32 ± 0.02 (16)	< 0.00001		
	R1441P	0.32 ± 0.03 (13)	< 0.00001		

[a] Values represent mean ± sem (number of measurements). The significance of the Student's *t*-test comparison, p, is against the WT.

a free parameter were statistically indistinguishable. We used this strategy routinely, in particular for $V_{rel} \leq 10$ mV.

To measure the time constant of the onset of inactivation for low-step depolarizations, which do not elicit appreciable currents (V_{rel} between -80 and -10 mV), we used the classical Hodgkin–Huxley type of double-pulse protocol. A conditioning prepulse of variable duration ($0.5 \leq t_c \leq 500$ ms) to the tested potential was followed by a 0.5 ms repolarization to -120 mV, that deactivated the noninactivated channels, and by a fixed test pulse to $V_{rel} \geq -10$. The peak response to the test pulse was plotted against t_c and fitted with a double-exponential function to estimate the time constants of M1 and M2 inactivation modes, τ_1 and τ_2. In some experiments, we also plotted the late mean test current (from 17 to 20 ms) versus t_c. As the late current is almost exclusively due to channels in the mode M2, these data were well fitted by a single exponential, with a time constant very similar to τ_2.

For more negative membrane potentials, we used a different protocol to estimate the time constant of recovery from inactivation. In this case, all channels were inactivated by a conditioning pulse of 150 ms at 0 mV, and tested for recovery of availability for activation after a variable period (1–500 ms) at the recovery potential between -140 and -100 mV (V_{rel} between -100 and -60) by a test pulse to $V \geq -20$ mV. The peak current response to the test pulse versus the duration of the recovery interval was fitted with a double-exponential function, yielding the time constants τ_1 and τ_2. As for the previous protocol, the fit of the late test current was well fitted by a single exponential with a time constant close to the estimated τ_2 from the fit of peak currents.

The kinetic properties of the bimodal inactivation of WT channels are shown in Fig. 5A. As discussed above, voltage dependencies are expressed as a function of relative voltages V_{rel}. Therefore, since the values of $V_{1/2}$ changed with time and from experiment to experiment, whereas the stimulation protocols were prepared for fixed values of V, the various data corresponded to widely scattered values of V_{rel} and were pooled in 10-mV bins for convenience of presentation. Horizontal and vertical bars represents, respectively, $\pm$ sem of V_{rel} and of the ordinate parameter in each bin. The continuous lines are best fits of the time constants of the two modes of inactivation according to Hodgkin–Huxley equations (Hodgkin and Huxley, 1952; Meves 1984):
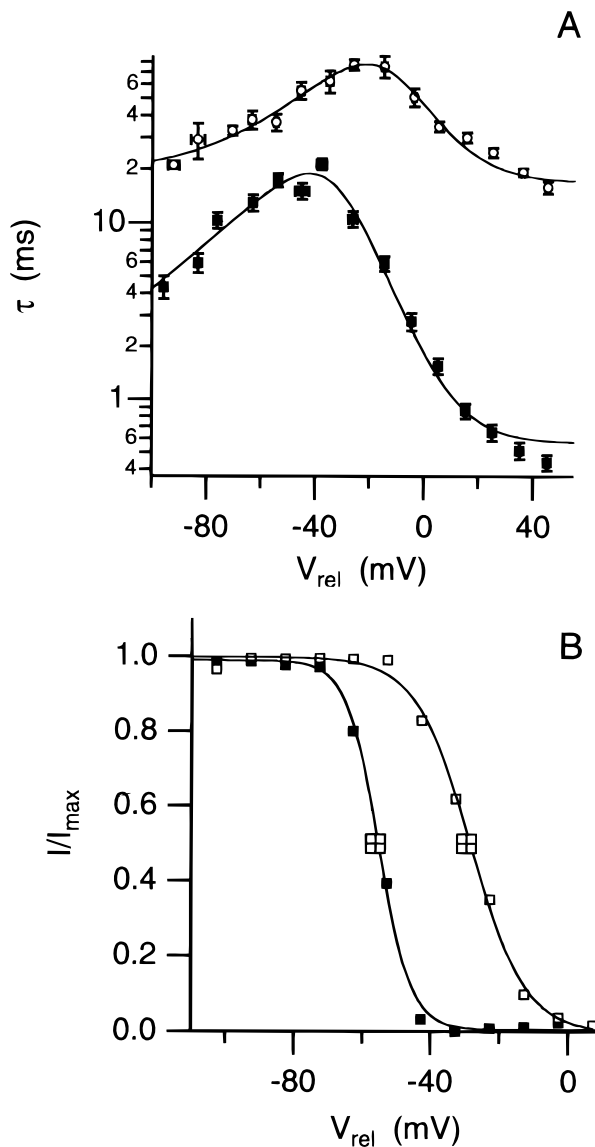

Fig. 5. (A) Inactivation kinetics of the WT sodium currents expressed in oocytes. The inactivation time constants of M1 mode, τ_1 (filled symbols), and the time constants of M2 mode, τ_2, (unfilled symbols), are plotted against V_{rel}. Data are the mean value of 3 to 20 measurements and are pooled in 10-mV bins. The continuous lines represent the best fits of data for a two-state Hodgkin–Huxley model. Observe the slower kinetics of inactivation of the mode M2 at any potential. (B) Steady-state voltage dependence of inactivation of mode M1 (filled symbols) and in mode M2 (unfilled symbols) measured in a representative experiment. The crossed squares represent the mean values of the half-inactivation potential from different experiments. The continuous lines are the best fits with a Boltzmann function.

$$\tau_i = (\alpha_i + \beta_i)^{-1}$$

$$\alpha_i = \frac{\alpha_i^{(0)}}{1 + e^{(V - V_\alpha)/k_\alpha}}$$

$$\beta_i = \frac{\beta_i^{((0)}}{1 + e^{-(V - V_\beta)/k_\beta}}$$

$$i = (1, 2)$$

Such accurate description is obviously model dependent and somewhat arbitrary, but was used here only for the purpose of obtaining empirical parameters that are well defined operationally and can be used for a fair quantitative comparison between mutants and WT properties. The phenotype changes introduced by the mutations studied here appear rather complicated (see below), but some general features that are likely most relevant for understanding the consequences of these changes on the phenomenology of muscle excitability stand out if we consider the two most important physiological ranges of membrane potentials: $0 \le V_{rel} \le 40$ mV (depolarized range) and $-80 \le V_{rel} \le -40$ mV (hyperpolarized range). Therefore, we have defined two operational parameters for each time constant-voltage curve, $\tau_{1,d}$ and $\tau_{2,d}$ in the depolarized range and $\tau_{1,h}$ and $\tau_{2,h}$ in the hyperpolarized range.

As mentioned earlier, the inactivation time constant of mode M2, τ_2, is larger than that of mode M1, τ_1, at any potential, and it achieves its maximum value at more positive potentials. The four operative parameters, $\tau_{1,d}$, $\tau_{2,d}$, $\tau_{1,h}$, and $\tau_{2,h}$ describing the properties of the time constants of inactivation of the two modes are given in Table II.

Steady-State Inactivation

The voltage dependence of steady-state inactivation at potentials near or below $V_{1/2}$ was measured with a double-pulse protocol. A 20-ms depolarizing test pulse to $V_{rel} \ge 0$ was preceded by 500-ms conditioning pulses to membrane potentials between -140 and -30 mV. The conditioning pulse was long enough to allow a steady-state probability of both the M1 and the M2 mode of inactivation since our estimates of time constant of the slow mode never exceeded 200 ms. Consistently prolonging the conditioning pulse up to 2 s did not significantly change the measured steady-state inactivation curve. We avoided routinely using such long prepulses, because they could induce slow inacti-

Table II. Average Inactivation Time Constants for Modes M1 (τ_1) and M2 (τ_2) Estimated Hyperpolarized Potential Range, HPR ($-80 \div -40$ mV), and Depolarized Potential Range, DPR ($0 \div 40$ mV)[a]

		$\tau_{1,h}$ (ms)	$\tau_{1,d}$ (ms)	$\tau_{2,h}$ (ms)	$\tau_{2,d}$ (ms)
	Wild type	13.9	0.9	39.4	26.3
PAM	S798F	19.7	1.4	74.9	51.2
	G1299E	41.7	1.4	133.7	43.3
	G1299V	12.9	1.8	81.9	76.4
	G1299A	17.1	1.0	107.0	49.0
HyPP	T698M	28.0	1.3	71.4	48.5
	M1353V	4.9	0.9	50.0	10.6
PC	T1306M	2.7	4.4	76.4	63.5
	R1441C	3.7	4.5	68.7	21.5
	R1441P	2.8	3.2	37.6	16.0

[a] These values were estimated from the fitting of the experimental data with the Hodgkin–Huxley-like equation.

vation processes with time constants of seconds (Cummins and Sigworth, 1996; Green et al., 1998; Hayward et al., 1997; Richmond et al., 1997; Rudy, 1978), that would accumulate and interfere with the characterization of the fast inactivation phenomena. The current elicited by the test pulse contained contributions from both gating modes. The contribution of mode M2 was estimated, in general, from the late current, between 17 and 20 ms from the onset of the test pulse when practically all the channels gating in mode M1 are fully inactivated [$\tau_1(V_{rel} \approx 0) < 3$ ms]. In the case of the PC mutants T1306M, R1441C, and R1441P, for which $\tau_1(V_{rel} \approx 0)$ is about 5 ms, the measure of the contribution of M2 was estimated between 23 and 30 ms. The M1 contribution to the total current was estimated from the difference between the peak and the late current. A conceptually better analysis, using the two amplitudes of the double-exponential fits to the test pulse response did not yield significantly different results. The voltage dependencies of M1 and M2 data were fitted by a Boltzmann function of the type:

$$I = \frac{I_{max}}{1 + e^{[(V_{rel} - V_h)/a]}}$$

The data shown later in Figs 5, 7, 9, and 11 were normalized to the fitted value of I_{max}. The mean values of the half-inactivation potentials and voltage–slope factors for each mode for WT and mutant channels are given in Table III.

As previously reported (Moran et al., 1998a), WT channels gating in the mode M1 inactivate at mem-

Table III. Steady-State Half-Inactivation Potential (V_{h1}, V_{h2}) and Voltage-Slope Factors (a_{h1}, a_{h2}) Measured for M1 and M2 Modes on rSkM1 Wild-Type and Mutant Channels[a]

		V_{h1} (mV)	a_{h1} (mV)	V_{h2} (mV)	a_{h2} (mV)
	Wild type	−56 ± 1 (15)	4.9 ± 0.1	−30 ± 1 (12)	8.0 ± 0.4
PAM	S798F	−47 ± 3 (9)	6.4 ± 0.2	−26 ± 2 (10)	5.0 ± 0.3
	G1299E	−50 ± 2 (11)	3.7 ± 0.1	−22 ± 2 (14)	7.0 ± 0.6
	G1299V	−48 ± 3 (9)	4.2 ± 0.2	−10 ± 3 (13)	7.3 ± 0.2
	G1299A	−48 ± 2 (12)	4.2 ± 0.2	−18 ± 1 (22)	6.3 ± 0.5
HyPP	T698M	−51 ± 1 (17)	5.0 ± 0.3	−34 ± 2 (14)	5.0 ± 0.3
	M1353V	−63 ± 3 (10)	5.0 ± 0.3	−50 ± 4 (10)	6.2 ± 0.5
PC	T1306M	−28 ± 2 (7)	6.7 ± 0.5	−13 ± 1 (6)	7.8 ± 0.3
	R1441C	−59 ± 3 (11)	11.7 ± 0.6	−54 ± 3 (13)	8.1 ± 0.4
	R1441P	−76 ± 13 (13)	11.6 ± 0.6	−61 ± 4 (8)	8.5 ± 0.5

[a] Values of V_h are refered to the half-activation potential ($V_{1/2}$) and represent mean ± sem (number of measurements).

brane potentials 27 mV more negative than when gating in mode M2 (Fig. 5B), consistently with the shift on the voltage dependence of the inactivation time constants. A larger shift of the same sign ($V_{h1} - V_{h2} \approx 75$ mV) has been reported by Ji *et al.* (1994) from experiments where P_{M2} was also significantly higher (~40%) than in our experiments (~10%). The estimates of V_{h1} and V_{h2} were obtained from the fit of the availability of total currents with a double Boltzmann function, without splitting the two components. Apart from this difference in the methodology, we do not have explanation for the discrepancy of results.

### Inactivation on PAM-Linked Mutations

Mean estimates of the two inactivation time constants of PAM-linked mutants as a function of V_{rel} are presented on Fig. 6. In each panel describing the properties of a particular mutation, the WT characteristics are also shown as dashed lines. We notice that, in the two ranges of physiological meaning analyzed, depolarized and hyperpolarized range, that larger phenotypic changes concern τ_2, which is always larger in the mutants and more so in the hyperpolarized range. Changes in the fast inactivating mode are barely significant in the depolarized range and insignificant in the hyperpolarized range for all mutants except for G1299E, which reaches a maximum value of τ_1 about threefold larger than normal at slightly more negative than a normal value of $V_{rel} \approx -40$ mV. Similar results have been reported for the human equivalents of these PAM mutants expressed in mammalian cells: in particular, the fast inactivation mode of S798F was studied

by Green *et al.* (1998), two inactivation time constants were characterized for G1299E, G1299V, and G1299A by Mitrovic *et al.* (1995), and mode M1 for G1299E, G1299V, and G1299A was studied by Hayward *et al.* (1996).

Changes of voltage dependence of steady-state inactivation were quite similar for all the PAM mutants. Representative experiments for each mutant are shown in Fig. 7, where the dashed lines refer to a representative experiment on WT channels. Data is characterized by the mean values of the half-inactivation potential indicated by crossed squares; the crossed circles give the mean for V_h values for the mutants.

Inactivation on HyPP-Linked Mutants

The two HyPP mutants that we studied do not show the same pattern of modifications of the modal inactivation. Mutant T698M showed only a slight increase on both inactivation time constants in the near subthreshold range of potentials and a more substantial increase (up to a factor of 2.5) for voltages above threshold or in the hyperpolarized range (Fig. 8A). Differently, mutant M1353V shows a large decrease of τ_1 up to a factor of 3.5 for $V_{rel} < 0$ mV and a similar decrease of τ_2 for $V_{rel} < -40$ mV (Fig. 8B). Variations introduced on τ_2 are also different between these mutants. The slower inactivation of mutant T698M is consistent with what has been described for the heterologous expression in mammalian cells of the same mutant (Cannon and Strittmatter, 1993) or of its human equivalent (Cummins *et al.*, 1993).
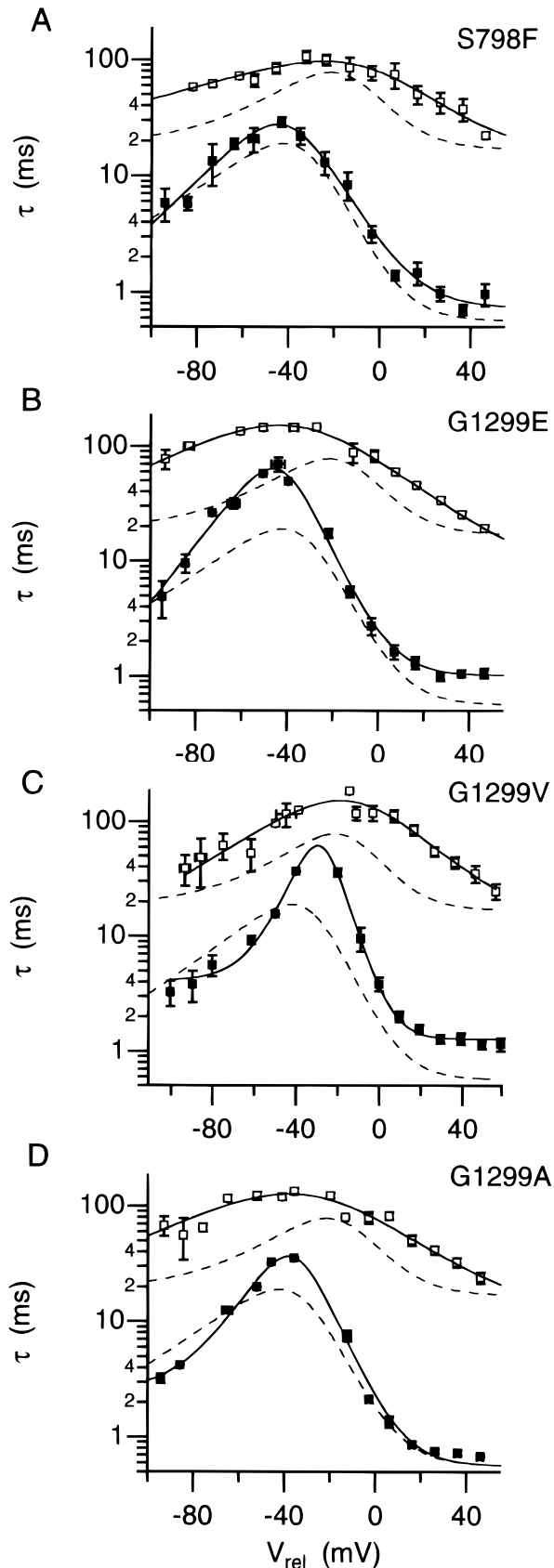
Changes in the steady-state inactivation curves showed a qualitatively similar pattern differentiation between the two HyPP mutants. For mutant T698M, V_{h2} is significantly shifted to negative potentials, whereas V_{h1} shows a slight opposite change. For mutant M1353V, both V_{h1} and V_{h2} are negatively shifted and the change of V_{h2} is very large (~ -20 mV) (Fig. 9). Interestingly, the different shifts of V_{h1} and V_{h2} result for both mutants in a significant increase in the difference ($V_{h2} - V_{h1}$) with respect to WT.

Inactivation on PC-Linked Mutants

The most consistent pattern of functional changes associated with myopathic mutations, also in relation to the predicted physiopathological consequences, are in the mode M1 inactivation kinetics of PC mutants (Fig. 10). For all three PC mutants studied, we find a drastic change in the voltage dependence of τ_1, which increases monotonically in the hyperpolarized range of potential and achieves a nearly constant value for $V_{rel} > -40$ mV. Consequently, it is about four- to fivefold smaller at hyperpolarized potentials and four- to fivefold larger at physiological depolarizations ($V_{rel} \geq 25$ mV). These effects, implying a slower inactivation during an action potential and a faster recovery during the interspike periods, are expected to cooperatively contribute to the increase in the tendency of muscle fibers to fire repetitively. The changes of τ_1, shown in Fig. 10, are similar to those reported for the human equivalent of mutants T1306M (Hayward *et al.*, 1996; Richmond *et al.*, 1997; Yang *et al.*, 1994), R1441C (Chahine *et al.*, 1994; Featherstone *et al.*, 1998; Ji *et al.*, 1996; Richmond *et al.*, 1997), and R1441P (Featherstone *et al.*, 1998) transfected in mammalian cells. Our analysis also shows alterations of the inactivation kinetics of mode M2. A twofold overall increase of τ_2 is observed for mutant T1306M (Fig. 10A). Differently, mutants R1441C and R1441P show a significant change on the voltage dependence of τ_2,

Fig. 6. Inactivation kinetics of the sodium currents expressed by the PAM-linked mutants (A) S798F (B) G1299E, (C) G1299V, and (D) G1299A. The inactivation time constants of M1 mode, τ_1 (filled symbols), and the time constants of M2 mode, τ_2 (unfilled symbols), are plotted against V_{rel}. Data are the mean value of 3 to 20 measurements and are pooled in 10-mV bins. The continuous lines represent the best fits of data for a two-state Hodgkin–Huxley model. The dashed lines are data obtained from WT channels for comparison.
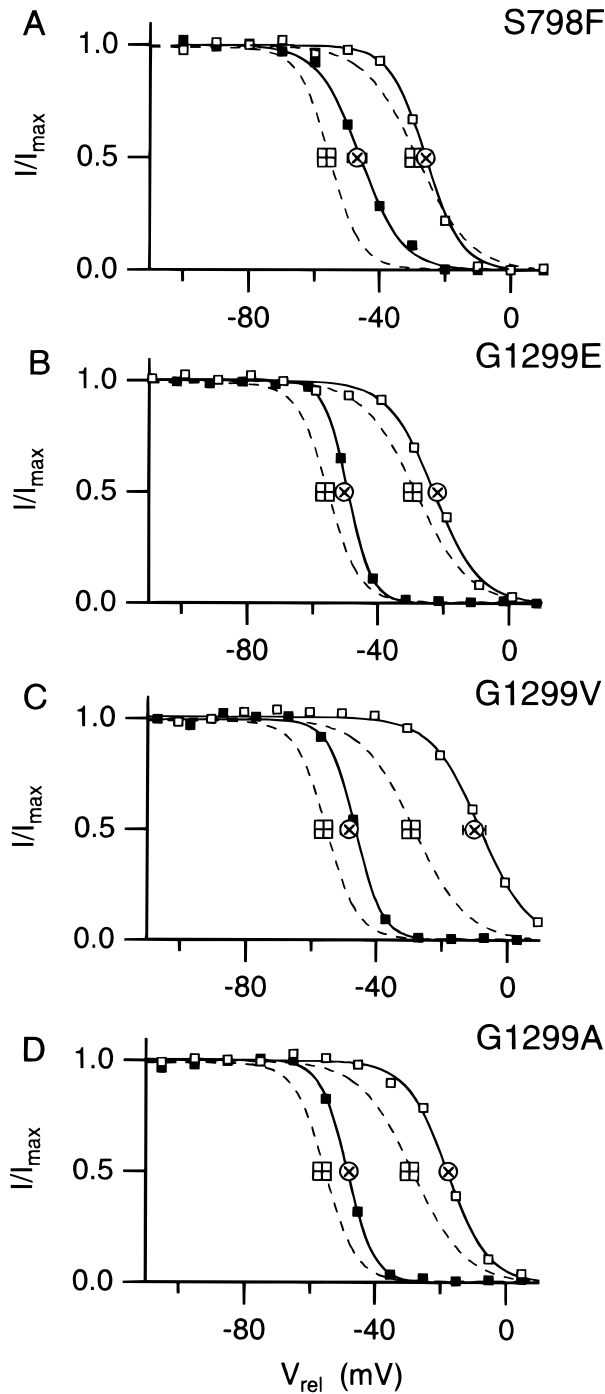
Fig. 7. Steady-state voltage dependence of inactivation of mode M1 (filled symbols) and in mode M2 (unfilled symbols) measured in representative experiments with sodium channel expressed by the PAM-linked mutants (A) S798F, (B) G1299E, (C) G1299V and (D) G1299A. The continuous lines are the best fits with a Boltzmann function. The dashed lines correspond to data obtained from WT channels, displayed on each panel for comparison. The crossed symbols represent the mean values of the half-inactivation potential from different experiments.
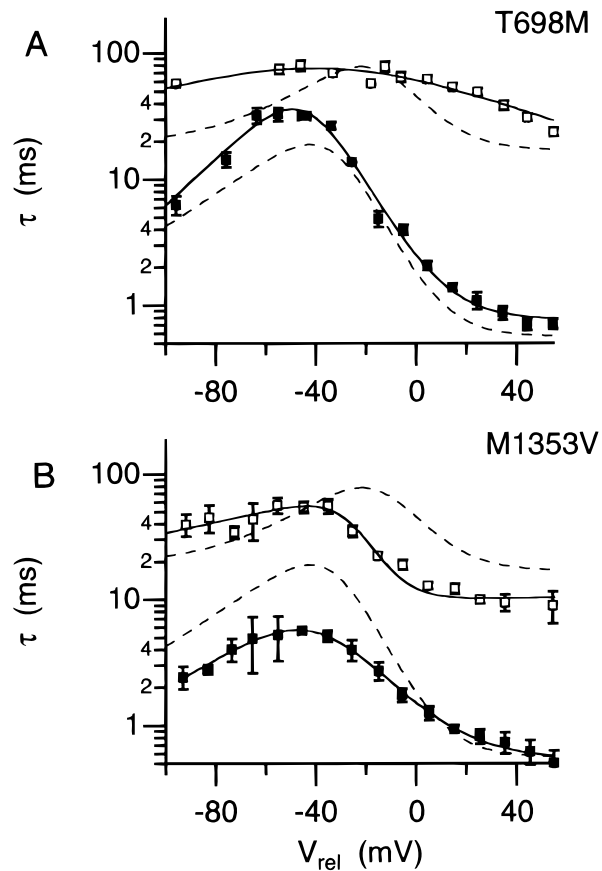

Fig. 8. Inactivation kinetics of the sodium currents expressed by the HyPP-linked mutants (A) T698M and (B) M1353V. The inactivation time constants of M1 mode, τ_1, (filled symbols), and the time constants of M2 mode, τ_2 (unfilled symbols), are plotted against V_{rel}. Data are the mean value of 3 to 20 measurements and are pooled in 10-mV bins. The continuous lines represent the best fits of data for a two-state Hodgkin–Huxley model. The dashed lines are data obtained from WT channels for comparison.

which decreases monotonically from a value higher than of WT at larger hyperpolarized potentials (four- to fivefold $V_{rel} \leq -60$ mV) to about the same of WT or slightly lower at superthreshold depolarization ($V_{rel} > 0$ mV) (Fig. 10B and C).

Even more marked differences between the three PC mutants are revealed by comparison of the steady-state inactivation curves (Fig. 11). In mutant T1306M, there is a large positive shift of V_{h1} (+25 mV), with roughly half as much in V_{h2}; in mutant R1441C, there is a large negative shift of V_{h2} (−25 mV), whereas V_{h1} is not significantly changed; R1441P shows a negative shift of V_{h1} that is accompanied by a very significant decrease of the steepness of the inactivation curve and a very large negative shift of V_{h2} with no change in
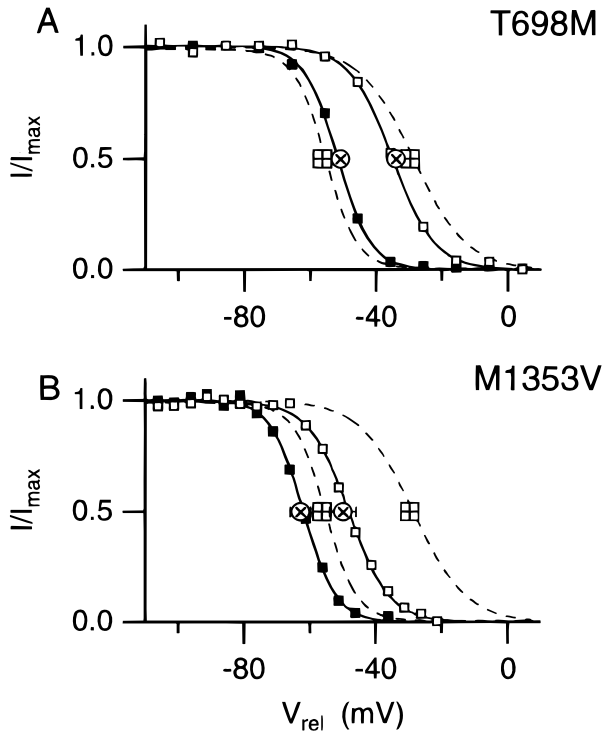
Fig. 9. Steady-state voltage dependence of inactivation of mode M1 (filled symbols) and in mode M2 (unfilled symbols) measured in representative experiments with sodium channel expressed by the HyPP-linked mutants (A) T698M and (B) M1353V. The continuous lines are the best fits with a Boltzmann function. The dashed lines correspond to data obtained from WT channels, displayed on each panel for comparison. The crossed symbols represent the mean values of the half-inactivation potential from different experiments.

slope. The qualitatively similar effect of the mutations is a similar reduction of the difference ($V_{h2} - V_{h1}$), which becomes almost zero in the case of mutant R1441C.

DISCUSSION

We have expressed WT and single-point mutants of the α subunit of rSkM1 channels linked with hereditary myopathies by cRNA injection in *Xenopus* oocytes. In all the cases, the currents mediated by these proteins have a double-exponential inactivation. This is consistent with the hypothesis that the channels are statistically distributed between two modes of gating—one with faster inactivation, mode M1, and a slower mode, M2, with an inactivation time constant more than tenfold larger (Ji *et al.*, 1994; Moorman *et al.*, 1990; Moran *et al.*, 1998a; Zhou *et al.*, 1991). We
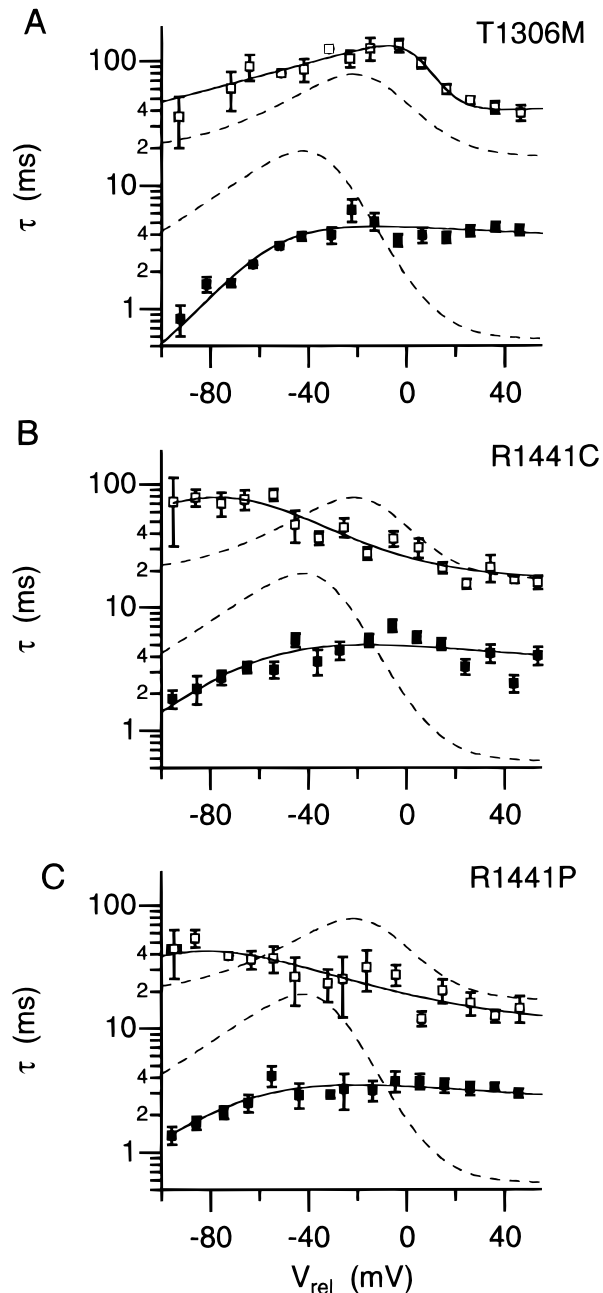

Fig. 10. Inactivation kinetics of the sodium currents expressed by the PC-linked mutants (A) T1306M, (B) R1441C, and (C) R1441P. The inactivation time constants of M1 mode, τ_1 (filled symbols), and the time constants of M2 mode, τ_2 (unfilled symbols) are plotted against V_{rel}. Data are the mean value of 3 to 20 measurements and are pooled in 10-mV bins. The continuous lines represent the best fits of data for a two-state Hodgkin–Huxley model. The dashed lines are data obtained from WT channels for comparison.
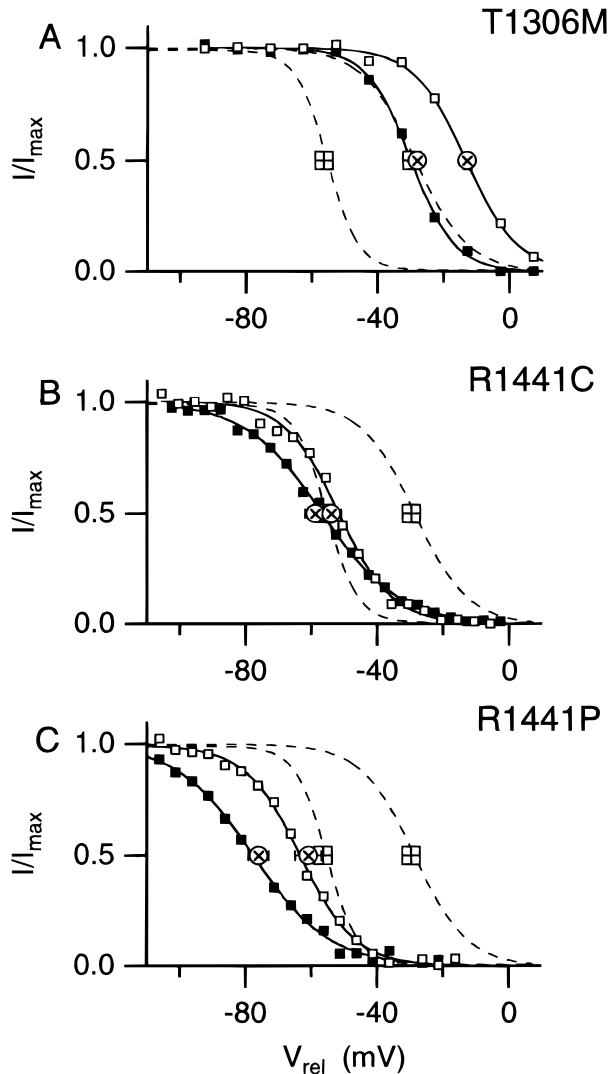
Fig. 11. Steady-state voltage dependence of inactivation of mode M1 (filled symbols) and in mode M2 (unfilled symbols) measured in representative experiments with sodium channel expressed by the PC-linked mutants (A) T1306M (B), R1441C, and (C) R1441P. The continuous lines are the best fits with a Boltzmann function. The dashed lines correspond to data obtained from WT channels displayed on each panel for comparison. The crossed symbols represent the mean values of the half-inactivation potential from different experiments.

have analyzed the functional changes introduced by myopathic mutations whose main effects have been reported to occur in the inactivation properties. These defects have been described to be both in terms of statistical analysis of the modal property and in terms of the voltage dependencies of the steady-state probability and kinetics of inactivation in the two separate gating modes. It has been shown by theoretical recon-

struction of the electrical behavior of the skeletal muscle that episodes of repetitive firing, occasionally followed by long inexcitable periods, and possibly at the origin of the myotonia and/or paralysis in patients affected by hereditary myopathies, may be explained by the presence of a very small fraction (0.0075) of sodium channels that do not inactivate (Cannon *et al.*, 1993a). The same type of analysis shows, however, that an increased proportion of channels that gate in mode M2 can also cause similar effects (Hayward *et al.*, 1996; Moran *et al.*, 1998a). The general qualitative results of these studies being in fact that many subtle changes in the inactivation properties of sodium channels can be the cause or contribute to pathological behavior of excitable tissues. Therefore, a more detailed description of the modal characteristics of the sodium channel inactivation and the analysis of the specific effects of the mutations on each gating mode could provide new insights for understanding the physiopathology of sodium channelopathies.

All the mutations studied in this work have already been studied in heterologous expression systems that purposely were chosen to be as close as possible to the native human system. Thus, many mutants were studied starting from the human α subunit hSkM1 and were expressed in mammalian cell lines and/or coexpressed with the β_1 subunit precisely with the purpose of depressing the gating mode M2 of the channels. These studies lead to the characterization of the sole mode M1 and mutational changes that increased the late currents during pulses of $10 \div 50$ ms duration were described as changes that caused sodium inactivation to become incomplete.

The result of our study is that we have measured the intrinsic properties of mode M2 and characterized this mode separately. We find that for all phenotypes, inactivation is complete and that the increase in P_{M2} is the cause of the apparent incompleteness of inactivation for relatively short pulses.

Independently of its use for better identifying the causes of hyperexcitability and apart from the relevance of mode M2 in the native tissue, there is also another important use of our studies. We are, in any case, characterizing a reproducible change in the gating behaviour of sodium channel mutation that could be some importance for studies of structure–function relations. We have used the heterologous expression of the rSkM1 channel in oocytes because the gating M2 mode has a much larger probability in this preparation, $P_{M2} \approx 10\%$ (Ji *et al.*, 1994; Moorman *et al.*, 1990; Moran *et al.*, 1998a, b; Trimmer *et al.*, 1989), whereas

the same channel expressed in mammalian cells behaves more similarly to the native preparation, with $P_{M2} < 0.3\%$ (Ukomadu *et al.*, 1992). This may be due to the coassembly with the sodium channels β_1 subunit that might be expressed endogenously in the embryonic human kidney cells used for transfection experiments (Mitrovic *et al.*, 1994). Indeed, the coexpression of the β_1 subunit in frog oocytes significantly reduces the M2 gating mode and makes the sodium currents more similar to those of the native muscle preparation (Cannon *et al.*, 1993b; Moran *et al.*, 1998b; Patton *et al.*, 1994). The different coexpression of α and β_1 subunits in embryonic kidney cells do not introduce substantial changes in the inactivation properties of the sodium channels (Hayward *et al.*, 1996). This reduces, however, the chances to obtain an accurate characterization of the M2 mode. When studying the effect of the coexpression of the β_1 subunit on the currents mediated by the WT or mutant T698M, G1299E, G1299V, G1299E, T1306M, and M1353V α subunits, we found that P_{M2} was reduced by about the same factor of three for these phenotypes, without significant changes of the voltage dependencies or the kinetics of inactivation in the two modes. This supports the assumption that the coassembly with the β_1 subunit merely increases the free energy of the M2 conformation of the α subunit. The expression of the sole α subunit allows a more quantitative comparison of the intrinsic properties for mode M2 on the various phenotypes and an accurate characterization of this mode without overlooking effects expected *a priori* from the β_1 subunit interaction which likely exist constitutively *in vivo*.

A major obstacle to quantitative studies of channels expressed heterologously is the large variability, two major types of which are observed. First, it is a general observation that patch–clamp measurements in most cell preparations show drift in the voltage dependencies of ion channel currents, likely due to changes of surface potentials, particularly at the cytoplasmic face of the cell membrane. Such drifts, first reported for measurements of sodium currents in chromaffin cells (Frenwick *et al.*, 1982), have been observed on HEK 293 cells permanently transfected with rSkM1 channels (Cummins and Sigworth, 1996) and are an invariable feature of patch–clamp measurements of sodium currents expressed by cRNA-injected oocytes (Moran *et al.*, 1998a, b, c; Shcherbatko and Brehm, 1998). The drifts must be obviously attributed to changes of the chemical and/or mechanical conditions of membrane solution arising from the dialysis

of the cytoplasm (in whole-cell or excised-patch configurations) and/or the modified interactions of membrane structures with cytoskeleton (Moran *et al.*, 1998a; Shcherbatko and Brehm, 1998). Because they are not observed during long experiments on whole oocytes with two-microelectrode voltage clamp (our observation, data not shown), without correcting for the drifts, comparative measurements of inactivation kinetics and of steady-state inactivation, or more generally of any voltage-dependent property, could be largely biased. The drifts can partially explain the contradictory results reported in the literature for the myopathic mutations of sodium channels studied in our present work. For example, the activation curve of the T698M channel has been described as either unchanged (Cannon and Strittmatter, 1993) or as shifted to negative potentials with respect to WT (Cummins and Sigworth, 1996; Cummins *et al.*, 1993) and, likewise, that of mutants G1299E, G1299V, and G1299A have been reported similar to WT (Hayward *et al.*, 1996) or negative shifted (Mitrovic *et al.*, 1995; Yang *et al.*, 1994).

An important methodology introduced in our analysis was to refer all potentials to that of half-activation of peak sodium currents, which we verified to be the same for the M1 and M2 mode (Moran *et al.*, 1998a, b, c), and which was measured periodically during the time course of any experiment. We found that the dependence of the gating properties on $V_{rel} = V - V_{1/2}$ obtained from different measurements on the same patch at different times and that referring our data to V_{rel} reduced the variability of the results from different experiments. Referring all potentials to $V_{1/2}$ prevents the measurements of possible shifts of the activation curves characterizing different phenotypes and, therefore, we cannot exclude that such shifts exist. However, our analysis of V_{rel} dependencies is operatively well defined and property, in particular the relative voltage dependencies of inactivation, processes that are most affected by the myopathic mutations.

The major source of variability that have to cope with in the study of modal behavior of inactivation of sodium channels concerns the probability of finding a channel, at one time at in any particular experiment, in either one of the two gating conformations. A wide variability of the modal propensity of any phenotype is observed in the oocyte expression system, both in measurements from different oocytes and in different measurements from the same patch at different times (Cummins and Sigworth, 1996; Moran *et al.*, 1998a; Zhou *et al.*, 1991). Clearly, a large source of variability

is again linked to the influence of chemical and mechanical changes in patch–clamp experiments, which are the only cases in which modal propensity changes during the experiment. However, a variable modal propensity is also observed in the whole oocyte, although no significant change occurs during voltage–clamp measurements of up to 1-h duration.

Intracellular factors modulating the modal propensity have so far remained elusive, whereas we can exclude redox potentials as being one of them (Moran *et al.*, 1998a). Explicit reports on the variability of modal propensity in measurements on transfected mammalian cells or in oocytes coinjected with α and β_1 subunits are not available, because most authors working with such preparations disregard the minor contribution to the currents by channels gating in mode M2. We have little experience on transfected cells preparations, but our experiments on coinjected oocytes also, indeed, show that the coassembly of the β_1 subunit merely reduces P_{M2}, but does not eliminate the variability. This observation is consistent with the idea that β_1 subunit decreases P_{M2} by a fixed factor but does not interfere with other factors that modulate the intrinsic propensity of the α subunit for either mode.

Because of the above discussed variability, for the characterization of changes in modal propensity associated with myopathic mutations expressed in oocytes, we had to depend on an accurate statistical analysis. In order to restrict the range of variability and to deal with a reasonably homogeneous sample of measurements for each phenotype, we decided to limit the measurements of modal propensity defined by P_{M2} only to the time interval of 3 to 5 min from the time at which the pipette come into contact with the oocyte membrane and the patch was exposed to the mechanical stress caused by the suction. Further cautions were taken regarding to the application of similar suction to induce the formation of the patch and the use of oocytes between 4 and 6 days after cRNA injection and the equilibration of oocytes for at least 20 min in the working solution before any measurement.

The results of our statistical analysis are that all mutant phenotypes show changes in modal propensity with high statistical significance. Indeed, the most simple and qualitative result of our study is a significant increase of the M2 current in all mutations studied, indicating that the mutant channels have two- to four-fold larger propensity to gate in the M2 mode (Table I). The increased intrinsic probability of the α-subunit

to adopt a conformation that slows the process of inactivation might be the most important functional change present in sodium channelopathies, because it predicts in all cases an increase of muscle excitability (Cannon *et al.*, 1993a; Moran *et al.*, 1998a) that is a common feature of patients with any of the various types of hereditary myopathies (Bulman, 1997; George, 1995; Hoffman *et al.*, 1995). Table I shows that for the expression of the sole α subunit in oocytes the mean value of 0.11 for P_{M2} in the wild-type phenotype is increased to values between 0.23 and 0.47 in all mutants and that the *p* values show that the phenotype changes have a very large degree of significance. The difficulty of studying P_{M2} changes in quasinormal conditions, in which the mode M2 contribution is small, is illustrated by our measurements on oocytes coinjected with α and β_1 subunits (columns 5 and 6, Table I). Not all phenotypes were studied by α–β_1 coinjection, but those that were showed an increase of P_{M2} with respect to the WT values similar to that observed with the sole α subunit. However, the $\sim$ fourfold lower value of P_{M2} decreases the accuracy of these measurements considerably and, consequently, the significance of the phenotypic changes, as shown in Table I. Thus, while the similarity of the phenotypical changes of P_{M2} measured with the sole α subunit or with the α–β_1 coinjection strongly supports the view that β_1 is merely reducing P_{M2} by a phenotype-independent factor, the sole consideration of the α–β_1 results would be scarcely sufficient for most mutants to conclude that P_{M2} significantly changes.

One enticing problem in the study of the sodium channel myopathies is that the general similarity of the defects observed, a slower and/or incomplete inactivation of the sodium currents, cannot be easily reconciled with the wide variability of the clinical features of the diseases. The purpose of this work was to provide a more detailed characterization of the inactivation properties of sodium channels, identifying particularly the mode M2 inactivation that seems hardly relevant for the gating of normal channels, but might play an important role in the myopathic physiopathology. The aimed goal was to find some new correlation between better characterized functional defect and the specific disease at which each mutation has been linked. This turned out to be a quite difficult task, as expected especially from the confused clinical descriptions of the different sodium channelopathies (see, for example, the OMIM database). Nevertheless, all the myotonic mutations studied here manifest modifications of the properties of both gating modes and some of the

changes that we have characterized seem to share a common pattern of correlation with the linked diseases.

The most characteristic phenotype among the three groups studied is that of the PC mutations. In these mutations, T1306M, R1441C, and R1441P, there is a clear common modification of the inactivation of the normally predominant mode M1 that has a faster recovery at negative potentials and a slower onset at depolarized voltages (see Fig. 10). However, the three PC mutants show different properties with respect to shifts of the voltage dependence of inactivation and the steepness of their voltage dependence (Fig. 11). These differences may be related to the different topological location of the mutated residues (extracellular on T1306M and intracellular on T1441C and R1441P), but it is interesting that overall effect in relation to the relative inactivation of the two modes is always a reduction on the difference between V_{h1} and V_{h2} (see Table III). In addition, in the HyPP-linked mutations, T698M and M1353V, there is a reduction of (V_{h2} − V_{h1}), that is mainly due to a negative shift of V_{h2} in M1353V and to a concomitant opposite shift of V_{h1} in T698M (Fig. 9). The increase of P_{M2} is also similar for the two mutations. The most distinguishing feature between the two is the change in activation kinetics: both modes are slowed in T698M, whereas the recovery from M1 inactivation and the onset of M2 inactivation are both hastened in M1353V. The common change observed in the PAM-linked mutations studied is a consistent general increase of τ_2 at all membrane potentials. Differences in mode M1 are barely significant for all PAM mutants. There is a positive shift of V_{h1} and V_{h2} (< 10 mV), whereas a slowing of the onset of M1 inactivation is significant in G1299V and G1299E and a slower recovery from mode M1 inactivation is highly significant for G1299E.

ACKNOWLEDGMENTS

REFERENCES

Auld, V. J., Goldin, A. L., Krafte, D. S., Marshall, J., Dunn, J. M., Catteral, W. A., Lester, H. A., Davidson, N., and Dunn, R. J. (1988). *Neuron* **1**, 449–61.

Barchi, R. L. (1995). *Annu. Rev. Physiol.* **57**, 355–385.
Bulman, D. E. (1997). *Human Mol. Genet.* **6**, 1679–1685.
Cannon, S. C. (1996a). *Annu. Rev. Neurosci.* **19**, 141–164.
Cannon, S. C. (1996b). *TINS* **19**, 3–10.
Cannon, S. C., and Corey, D. P. (1993). *J. Physiol.* **466**, 501–520.
Cannon, S. C., and Strittmatter, S. M. (1993). *Neuron* **10**, 317–326.
Cannon, S. C., Brown, R. H., and Corey, D. P. (1991). *Neuron* **6**, 619–626.
Cannon, S. C., Brown, R. H., and Corey, D. P. (1993a). *Biophys. J.* **65**, 270–288.
Cannon, S. C., McClatchey, A. I., and Gusella, J. F. (1993b). *Pflügers Arch.* **423**, 155–157.
Chahine, M., George, A. L., Zhou, M., Ji, S., Sun, W., Barchi, R. L., and Horn, R. (1994). *Neuron* **12**, 281–94.
Chang, S. Y., Satin, J., and Fozzart, H. A. (1996). *Biophys. J.* **70**, 2581–2592.
Cummins, T. R., and Sigworth, F. J. (1996). *Biophys. J.* **71**, 227–236.
Cummins, T. R., Zhou, Y., Sigworth, F. J., Ukomadu, C., Stephan, M., Ptacek, L. J., and Agnew, W. S. (1993). *Neuron* **10**, 667–678.
DeSilva, S. M., Kuncl, R. W., Griffin, J. W., Cornblath, D. R., and Chavoustie, S. (1990). *Nerve Muscle* **13**, 21–26.
Featherstone, D. E., Fujimoto, E., and Ruben, P. C. (1998). *J. Physiol.* **406**, 627–638.
Frenwick, E., Marty, A., and Neher, E. (1982). *J. Physiol.* **331**, 599–635.
George, A. L. (1995). *Kidney Intern.* **48**, 1180–1190.
Green, D. S., George, A. L., and Cannon, S. C. (1998). *J. Physiol.* **510**, 685–694.
Hamill, O., Marty, A., Neher, E., Sakmann, B., and Sigworth, F. (1981). *Pflügers. Arch.* **391**, 85–100.
Hayward, L. J., Brown, R. H., Jr., and Cannon, S. C. (1996). *J. Gen. Physiol.* **107**, 559–576.
Hayward, L. J., Brown, R. H., Jr., and Cannon, S. C. (1997). *Biophys. J.* **72**, 1204–1019.
Hille, B. (1992). *Ionic Channels of Excitable Membranes.* Sinauer, Sunderland, MA.
Hodgkin, A. L., and Huxley, A. F. (1952). *J. Physiol.* **117**, 500–44.
Hoffman, E. P., Lehmann-Horn, F., and Rüdel, R. (1995). *Cell* **80**, 681–686.
Ji, S., Sun, W., George, A. L., Jr., Horn, R., and Barchi, R. L. (1994). *J. Gen. Physiol.* **104**, 625–643.
Ji, S., George, A. L., Horn, R., and Barchi, R. L. (1996). *J. Gen. Physiol.* **107**, 183–194.
Kudel, T. A. (1985). *Proc. Natl. Acad. Sci. USA* **82**, 488–492.
Lehmann-Horn, F., Iaizzo, P. A., Hatt, H., and Franke, C. H. (1991). *Pflügers Arch.* **418**, 297–299.
Lerche, H., Heine, R., Pika, U., George, A., Mitrovic, N., Browatzki, M., Weiss, T., Rivet-Bastide, M., Franke, C., Lomonaco, M., Ricker, K., and Lehmann-Horn, F. (1993). *J. Physiol.* **470**, 13–22.
Lerche, H., Mitrovic, N., Dubowitz, V., and Lehmann-Horn, F. (1996). *Ann. Neurol.* **39**, 599–608.
Liman, E. R., Tytgat, J., and Hess, P. (1992). *Neuron* **9**, 861–871.
Meves, H. (1984). In *Current Topics in Membranes and Transport: The squid axon: Hodgkin–Huxley: Thirty Years After* (Baker, P. eds.), Academic Press, New York, pp. 279–329.
Mitrovic, N., George, A. L. J., Heine, R., Wagner, S., Pika, S., Hartlaub, U., Zhou, M., and Lerche, H. (1994). *J. Physiol.* **478**, 395–402.
Mitrovic, N., George, A. L., Lerche, H., Wager, S., Falke, C., and Lehmann-Horn, F. (1995). *J. Physiol.* **487**, 107–114.
Moorman, J. R., Kirsch, G. E., VanDongen, A. M. J., Joho, R. H., and Brown, A. M. (1990). *Neuron* **4**, 243–52.
Moran, O., Nizzari, M., and Conti, F. (1998a). In *Neuronal Circuits and Networks: Modal Gating of Sodium Channels and Possible Physiological Implications on Hereditary Myopathies* (Torre, V. and Nicolls, J., eds.), Springer Verlag, Berlin, pp. 3–19.

Moran, O., Melani, R., Nizzari, M., and Conti, F. (1998b). *J. Bioenerg. Biomemb.* **30**, 579–588.

Moran, O., Nizzari, M., and Conti, F. (1998c). *Biophys. Biochem. Res. Commun.* **246**, 792–796.

Patton, D. E., Isom, L. L., Catterall, W. A., and Goldin, A. L. (1994). *J. Biol. Chem.* **269**, 17640–17655.

Richmond, J. E., Featherstone, D. E., and Ruben, P. C. (1997). *J. Physiol.* **499**, 589–600.

Rudy, B. (1978). *J. Physiol.* **283**, 1–21.

Sanger, F., Nicklen, S., and Coulson, A. R. (1977). *Proc. Natl. Acad. Sci. USA* **74**, 5463–5467.

Shcherbatko, A., and Brehm, P. (1998). *Biophys. J.* **74**, A394.

Stämpfli, R., and Hille, B. (1976). In *Frog Neurobiology*: Electrophysiology of the Peripheral Myelinated Nerve. (Llinás, R. and Precht, W., eds.), Springer Verlag, Berlin, pp. 1–32.

Stühmer, W. (1992). In *Methods in Enzymology: Ion Channels: Electrophysiological Recording of Xenopus Oocytes* (Rudy, B. and Iverson, L. E., eds.), Academic Press, New York pp. 319–339.

Sugimoto, M., Esaki, N., Tanaka, H., and Soda, K. (1989). *Anal. Biochem.* **179**, 309–311.

Tahmoush, A. J., Schaller, K. L., Zhang, P., Hyslop, T., Heiman-Patterson, T., and Caldwell, J. H. (1994). *Neuromusc. Disorders* **4**, 447–454.

Trimmer, J. S., Cooperman, S. S., Tomiko, S. A., Zhou, J., Crean, S. M., Boyle, M. B., Kallen, R. G., Sheng, Z., Barchi, R. L., Sigworth, F. J., Goodman, R. H., Agnew, W. S., and Mandel, G. (1989). *Neuron* **3**, 33–49.

Ukomadu, C., Zhou, J., Sigworth, F. J., and W. S., Agnew (1992). *Neuron* **8**, 663–676.

Wend, D. J., Starmer, C. F., and Grant, A. O. (1992). *Amer. J. Physiol.* **263**, C1234–C1240.

Yang, N., Ji, S., Zhou, M., Patcek, L. J., Barchi, R. L., Horn, R., and George, A. L. J. (1994). *Proc. Natl. Acad. Sci. USA* **91**, 12785–12789.

Zhou, J., Potts, J. F., Trimmer, J. S., W. S., Agnew, and F. J., Sigworth (1991). *Neuron* **7**, 775–785.